MDPI

Article

Energy Management Control Strategy for Saving Trip Costs of Fuel Cell/Battery Electric Vehicles

Juhui Gim [1], Minsu Kim [2] and Changsun Ahn [2,*]

1   School of Electrical, Electronic and Control Engineering, Changwon National University, Changwon 51140, Korea; juhuigim1992@gmail.com
2   School of Mechanical Engineering, Pusan National University, Busan 46241, Korea; kmsms5051@gmail.com
*   Correspondence: sunahn@pusan.ac.kr

Abstract: Fuel cell vehicles (FCVs) should control the energy management between two energy sources for fuel economy, using the stored energy in a battery or generation of energy through a fuel cell system. The fuel economy for an FCV includes trip costs for hydrogen consumption and the lifetime of two energy sources. This paper proposes an implementable energy management control strategy for an FCV to reduce trip costs. The concept of the proposed control strategy is first to analyze the allowable current of a fuel cell system from the optimal strategies for various initial battery state of charge (SOC) conditions using dynamic programming (DP), and second, to find a modulation ratio determining the current of a fuel cell system for driving a vehicle using the particle swarm optimization method. The control strategy presents the on/off moment of a fuel cell system and the proper modulation ratio of the turned-on fuel cell system with respect to the battery SOC and the power demand. The proposed strategy reduces trip costs in real-time, similar to the DP-based optimal strategy, and more than the simple energy control strategy of switching a fuel cell system on/off at the battery SOC boundary conditions even for long-term driving cycles.

1. Introduction

The depletion of limited fossil fuels and pollution caused by fossil energy usage have forced the fuel economy and exhaust gas regulations, presenting a new generation for eco-friendly and high-efficiency vehicles that alternate fossil energy to electric energy [1]. The mainstream of electric vehicles is the battery electric vehicle (BEV) which uses the stored electricity in batteries. However, battery performance remains insufficient as an alternative to internal combustion engine (ICE) vehicles, owing to short driving distances and long charging times [2]. Recently, a fuel cell technology generating electricity from hydrogen (H_2) is being highlighted to compensate for the aforementioned battery problems [3].

A fuel cell vehicle (FCV) reduces the battery size by self-generating electricity, increases driving distance (100 km per 1 kg hydrogen [4]), and requires a short charging time by charging hydrogen, instead of electricity. Therefore, an FCV can be the new-generation vehicle that can satisfy requirements for eco-friendly driving performance. The problem of an FCV is an energy management strategy (EMS) between a battery and a fuel cell, i.e., deciding whether to use stored electricity in a battery or to generate electricity with a fuel cell system [5,6]. The EMS determines the fuel efficiency and fuel cell operating efficiency, which affects the required battery power and battery size. The optimal EMS for an FCV typically focuses on the efficient operating range of the fuel cell and the optimization of battery sizing [5–9].

Another consideration for EMS is cost and fuel cell/battery lifetime. The cost of hydrogen varies dramatically depending on the production method and distribution distance [10]. Moreover, the cost per mile of hydrogen is 2–3 times greater than gasoline. In

addition, the frequent on/off cycles of a fuel cell system causes accelerated aging of fuel cell stacks, which account for approximately 66% of the cost of the fuel cell system based on 1000 produced annually [11]. On the other hand, overcharge/over-discharge, charging a battery with a high current, and additional resulting temperature changes degrade the battery lifetime despite reducing repeated operation of the fuel cell system and hydrogen usage [12]. The associated cost and lifetime increase the overall expense for driving an FCV, i.e., trip cost. Therefore, an efficient energy management control strategy between using hydrogen and using stored electricity in a battery is required to reduce trip costs.

The best energy-optimal strategy, i.e., the optimal fuel cell system on/off strategy, can be defined as the overall optimal solution of global optimization-based methods for a given total driving profile. However, the best fuel-optimal strategy of the global optimization methods is usually utilized as a benchmark because of non-causality requiring the full driving profile [13–15]. Therefore, researchers use two methods for control strategies in real-time. The first method is to extract the rules from trends of the best energy-optimal strategy [7,8,16–19], and the second method is to adopt implementable optimal control algorithms in real-time [9,18–21]. The general practical application employs the rule-based method because of lower computational requirements than the second method. An issue of the rule-based method is the extraction of the rule guaranteed to cover the trend of the optimal solution for various driving conditions. However, most research has designed rule-based control strategies in terms of minimizing power loss [19], optimizing battery size [7,8], or optimizing fuel usage [16–18], but not in terms of trip costs involving the hydrogen cost and subsystem obsolescence.

This paper proposes a practical energy management control strategy for an FCV reducing trip costs. The proposed control strategy is extracted from analyzing the best energy-solution of the dynamic programming (DP), one of the global optimization methods. The cost of the DP is designed as a function of cost with respect to hydrogen usage and fuel cell/battery lifetime for reducing the trip cost. The DP extracts the best energy-optimal modulation ratio between alternate usage of stored electricity in a battery and the generated electricity by a fuel cell system. The trend of the fuel cell system's allowable current is analyzed in terms of the required power demand and the current battery state of charge (SOC), and the best modulation ratio operating the fuel cell system is defined using the particle swarm optimization (PSO) method from the allowable current of the fuel cell system and fuel cell system dynamics. Finally, the practical fuel cell operation is defined as a function of the battery SOC. The extracted control strategy is validated by comparing the DP-based optimal strategy with the simple EMS of turning the fuel cell system on and off at the battery state. The designed strategy reduces trip costs, similar to the DP-based optimal strategy even without prior knowledge of future vehicle speed and significantly more than the simple EMS even for long-time driving conditions. Therefore, the designed control strategy can be implemented as a controller that reduces trip cost in real-time, taking into account cost-effective hydrogen usage while minimizing the two factors that accelerate the obsolescence of a fuel cell system and a battery: frequent on/off cycling of a fuel cell system and overcurrent in a battery.

Section 2 describes the fuel cell vehicle model; Section 3 extracts the energy management strategy based on the DP; Section 4 discusses the simulation results; and, Section 5 finishes with a number of conclusions.

2. Fuel Cell Vehicle Model

The target fuel cell vehicle is based on the FC/battery model distributed at the IEEE VTS Motor Vehicles Challenge 2017 held at the IEEE vehicle power and propulsion conference (IEEE VPPC) [22]. The FCV structure consists of three subsystems; a fuel cell system including the unidirectional DC/DC converter, a battery, and a motor-based traction subsystem, as shown in Figure 1. Each system is simplified to a control-oriented model. Table 1 lists the parameters and their values for the FCV model.
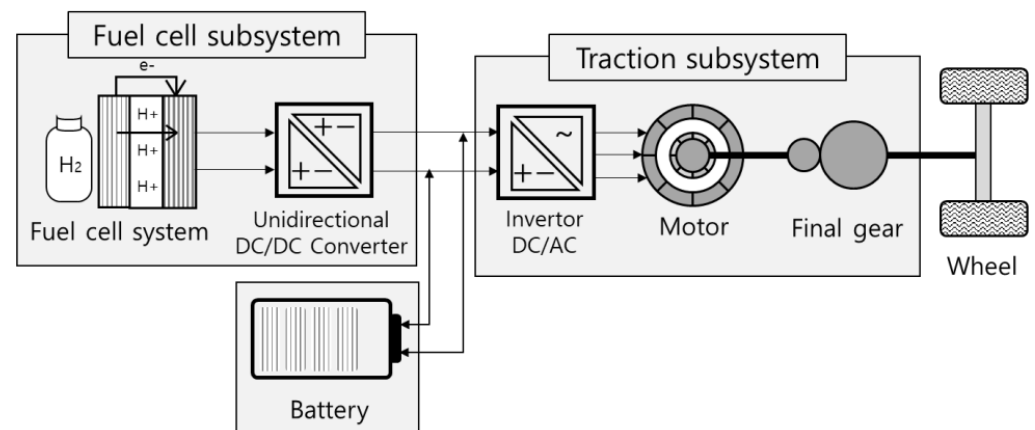
Figure 1. Fuel cell vehicle structure: Thin lines indicate electrical connections, and thick lines indicate mechanical connections.

Table 1. Parameters for the fuel cell vehicle model.

Subsystem	Symbol	Parameter	Value
Fuel cell subsystem (16 kW, 40–60 V PEMFC)	R_s	Resistance of the smoothing inductor	5 mΩ
	L_s	Inductance of the smoothing inductor	0.25 mH
	$\eta_{chopper}$	Boost chopper efficiency	95%
Battery (80 V–40 Ah LiFePO4)	R_{batt}	Series internal resistance of the battery	0.028 Ω
	R_{batt1}	Resistance of the battery	0.1417 Ω
	C_{batt1}	Capacitance of the battery	3529.4 F
	Q_{batt}	Battery capacity	40 Ah
Vehicle traction subsystem	M_v	Vehicle mass	698 kg
	ρ	Air density	1.2230 kg/m^3
	C_d	Air drag coefficient	0.7
	A	Frontal area of the vehicle	1 m^2
	g	Gravitational acceleration	9.81 m/s^2
	f	Rolling resistance coefficient	0.02

- Fuel cell subsystem;

A fuel cell system is based on a 16 kW, 40–60 V, proton exchange membrane fuel cell (PEMFC) with a maximum current of 400 A. A complex fuel cell system is modeled as an equivalent voltage source with respect to the current of the fuel cell using a quasi-static model experimentally validated, as shown in Figure 2a. The hydrogen consumption represents the hydrogen mass flow with respect to the current of the fuel cell, as shown in Figure 2b. The hydrogen state of charge (SOC_{H2}) is estimated by the hydrogen mass flow rate counting:

$$SOC_{H_2} = \frac{m_{H_2,init} - \int \dot{m}_{H_2} i_{fc} dt}{m_{H_2,init}}, \tag{1}$$

where $m_{H_2,\,init}$ is the initial mass of the hydrogen, $\dot{m}_{H_2}$ is the hydrogen mass flow rate, and i_{fc} is the current of the fuel cell system.
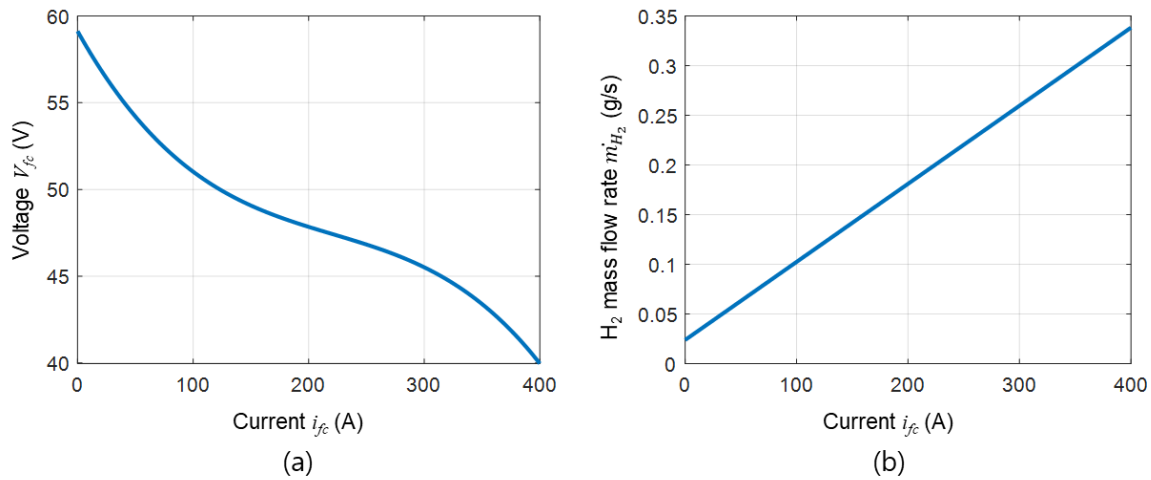
Figure 2. Fuel cell system modeling: (**a**) Fuel cell model; (**b**) Hydrogen consumption model.

The fuel cell system is connected to the unidirectional DC/DC converter to control the generated current by the fuel cell system. The unidirectional DC/DC converter is modeled simply as a combination of a smoothing inductor and an irreversible boost chopper. The smoothing inductor is designed as the first-order RL circuit model approximated by the first-order Euler's method. The irreversible boost chopper regulates the voltage level between the fuel cell system and the battery, allowing energy generated by the fuel cell system to flow towards the vehicle traction subsystem:

$$
\begin{aligned}
i_{fc}(t+1) &= \left(1 - \frac{R_s}{L_s}\Delta t\right)i_{fc}(t) + \frac{1}{L_s}\Delta t\left(V_{fc} - V_{chopper}\right), \\
V_{chopper} &= m_{fc}V_{batt}, \quad where, \; P_{demand} > 0, \\
i_{chopper} &= m_{fc}i_{fc}\eta_{chopper}, \quad where, \; P_{demand} > 0,
\end{aligned}
\tag{2}
$$

where V_{fc}, $V_{chopper}$, and V_{batt} are the voltage of the fuel cell system, the boost chopper, and the battery, respectively. $i_{chopper}$ represents the current of the boost chopper. $V_{chopper}$ and $i_{chopper}$ are irreversible with respect to the power demand of a vehicle P_{demand}. m_{fc} is the modulation ratio controlling current in the fuel cell system. The modulation ratio ranges from 0–1, and the zero modulation ratio denotes that the fuel cell system is fully operated. Δt is the discretized time.

- Battery;

The battery is based on an 80 V–40 Ah Lithium Iron Phosphate (LiPePO4) battery pack. The control-oriented battery model uses the first-order RC equivalent circuit model consisting of an open circuit voltage V_{OC}, a series internal resistance R_{batt0}, and a parallel combination of resistance R_{batt1} and capacitance C_{batt1}:

$$
\begin{aligned}
i_{batt} &= \frac{V_{OC} - R_{batt0} - V_{batt}}{R_{batt1}} + C_{batt1}\frac{d}{dt}\left(V_{OC} - R_{batt1}i_{batt} - V_{batt}\right), \\
V_{batt} &= \frac{\left(V_{OC} + \sqrt{V_{OC}^2 - 4\cdot P_{batt}\cdot r_{batt0}}\right)}{2}, \\
P_{batt} &= P_{tract} - \eta_{chopper}\cdot i_{fc}\left(V_{fc} - i_{fc}R_s\right),
\end{aligned}
\tag{3}
$$

where i_{batt} and V_{batt} are the current and voltage of the battery, respectively. P_{batt} and P_{tract} are the battery power and transmission power to drive the vehicle. V_{OC} is the function of the battery state of charge (SOC_{batt}). The SOC_{batt} is estimated by the column counting from the initial battery SOC $SOC_{batt,\,init}$:

$$
SOC_{batt} = SOC_{batt,init} - \frac{1}{Q_{batt}}\int i_{batt}dt.
\tag{4}
$$

The battery operates a motor of the vehicle traction subsystem by flowing the stored current to the DC/AC inverter. On the other hand, the battery can be charged by the fuel cell system through the DC/DC converter or by regenerating through the DC/AC inverter.

- Traction subsystem;

A traction system consists of a DC/AC inverter and a motor-to-wheel drive system. The currents from two energy sources, the battery and the fuel cell subsystem, feed the motor-to-wheel drive system through a 15 kW DC/AC inverter:

$$i_{tract} = i_{batt} + i_{chopper}, \tag{5}$$

where i_{tract} is the required current to tract the vehicle.

A vehicle is designed by considering only longitudinal dynamics for vehicle speed v_v, consisting of traction force F_{tract} and resistance force F_{resis} by aerodynamics, rolling resistance, and road grade:

$$\begin{aligned} M_v \dot{v}_v &= F_{tract} - F_{resis}, \\ F_{resis} &= \tfrac{1}{2}\rho C_d A v_v^2 + M_v g f + M_v g \theta, \end{aligned} \tag{6}$$

where θ is the road grade. The positive traction force requires the current to tract the vehicle i_{tract}. The relationship between i_{tract} and F_{tract} is simplified using η_{tract}:

$$i_{tract} V_{batt} = P_{tract} = \frac{P_{demand}}{\eta_{tract}} = \frac{F_{tract} v_v}{\eta_{tract}}, \tag{7}$$

where P_{demand} and P_{tract} are the power demand with respect to the vehicle speed v_v and electrical power at the transmission to traction the vehicle, respectively. η_{tract} is an experimentally validated quasi-static model associated with both the conversion efficiency between electrical and mechanical energies and the dynamics of the invertor-to-wheel mechanical transmission system, as shown in Figure 3.
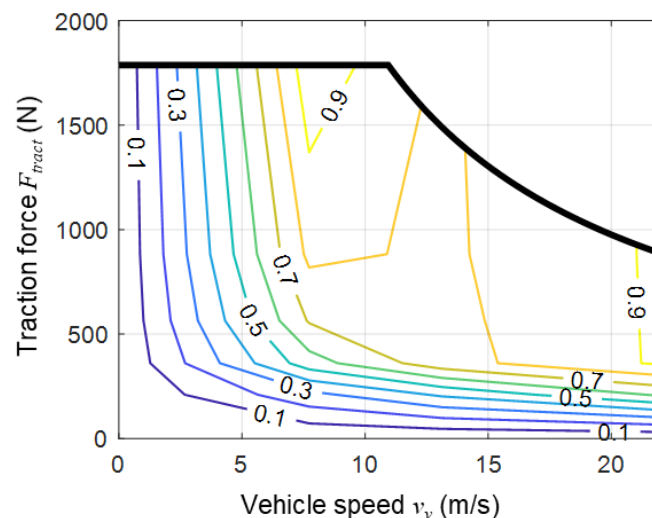
Figure 3. η_{tract} model.

3. Design of Energy Management Control Strategy

The energy management control strategy for reducing the trip cost is extracted in following three steps: (1) Design the DP structure for the optimal EMS to save trip cost; (2) Analyze trends of the optimal EMS; and, (3) Design the control strategy to implement the optimal EMS trends. The control strategy aims to achieve real-time performance similar to the DP-based optimal EMS utilizing the total driving cycle while exhibiting robustness to various speed conditions.

3.1. Design of the Dynamic Programming

The DP is a numerical solver that finds a globally optimal solution by decomposing a sequence of decision steps over time [23]. The DP calculates transition costs for all states backward from the final state, then recovers the decision to minimize the cost from the given initial states. Therefore, the optimal solution by the DP can be the full potential for the initial states.

Let us describe the FCV model as the nonlinear state-space model for the optimal EMS:

$$\dot{\mathbf{x}} = f(\mathbf{x}, u, d),$$
$$\mathbf{x} = \begin{bmatrix} i_{fc} & SOC_{batt} \end{bmatrix}^T, \ u = m_{fc}, \ d = F_{tract}. \tag{8}$$

where the traction force F_{tract} is the function of the vehicle speed v_v. The optimal EMS is to find the optimal input u^*, i.e., the optimal modulation ratio of the fuel cell m_{fc}^*, that minimizes the cost function associated with the trip costs for the total driving time $[t_0, t_f]$:

$$m_{fc}* = \underset{m_{fc}}{\mathrm{argmin}} \left[\sum_{t_0}^{t=t_f} \{ J(\mathbf{x}(t), u(t), d(t)) \} \right],$$
$$s.t. \ \dot{\mathbf{x}} = f(\mathbf{x}, u, d), \ g(x, u) \le 0, \ h\left(x(t_0), x(t_f) \right) = 0, \tag{9}$$

where $J(\mathbf{x}(t), u(t), d(t))$ is the cost function to use the input u at the state $\mathbf{x}$ with the traction force demand d at time t. $g(x, u)$ is an algebraic inequality constraint, and $h(x(t_0), x(t_f))$ is a boundary condition.

A cost function $J(\mathbf{x}(t), u(t), d(t))$ for the optimal EMS reducing the trip cost takes into account the trip cost with respect to hydrogen consumption, the fuel cell system lifetime, and the battery lifetime:

$$J = J_{H_2} + J_{FC} + J_{batt}, \tag{10}$$

where J is represented as the price by defining J_{H2} as the price with respect to hydrogen consumption and defining J_{FC} and J_{batt} as the replacement price with respect to the degradation of a fuel cell system or battery.

The cost for hydrogen consumption J_{H2} is proportional to the amount of hydrogen consumed during driving:

$$J_{H_2} = \$_{H_2} \cdot \sum_{t=t_0}^{t=t_f} \dot{m}_{H_2} \Delta t, \tag{11}$$

where $\$_{H2}$ is the market price of hydrogen per 1 kg.

A cost for the fuel cell system lifetime J_{FC} is proportional to the degradation of the fuel cell system due to frequent on/off cycling and heavy use of power [11]:

$$J_{FC} = \$_{FC} \cdot \frac{1}{T_{FC}} \cdot \left[w_{switch} N_{switch} + w_{power} \sum_{t=t_0}^{t} \left\{ \left(1 + \frac{w_{perror}}{\overline{P}_{fc}} \left(P_{fc}(t) - \overline{P}_{fc} \right)^2 \right) \Delta t \right\} \right], \tag{12}$$

where N_{switch} is the number of switching on of the fuel cell system. The switching on is defined when the current of the fuel cell i_{fc} exceeds 1 mA. w_{switch} is the degradation coefficient with respect to the switching on of the fuel cell system. w_{power} and w_{perror} are the load coefficients for the degradation with respect to heavy power. P_{fc} is the power of the fuel cell system at the time t, and $\overline{P}_{fc}$ is the nominal power of the fuel cell system. T_{FC} is the lifetime of the fuel cell system for normalizing the performance degradation associated with the switching on/off and heavy power. $\$_{FC}$ is the market price of the 16 kW fuel cell system.

A cost for the battery lifetime J_{batt} depends on the battery SOC and power transients because high currents, especially high recharge currents, accelerate battery degradation [24]:

$$J_{batt} = \$_{batt} \cdot \frac{1}{Q_{batt,max}} \cdot \sum_{t=t_0}^{t=t_f} \left[\left| i_{batt}(t) \cdot \left\{ 1 + w_{SOC_{batt}}(1 - SOC_{batt}(t))^2 \right\} \cdot \left\{ 1 + w_{charge} \frac{|i_{batt}(t)|}{Q_{batt}} \right\} \right| \cdot \Delta t \right], \qquad (13)$$

where i_{batt} and SOC_{batt} are the current and battery SOC at the time t, respectively. $w_{SOCbatt}$ and w_{charge} are the degradation coefficient with respect to battery SOC and overcurrent. $Q_{batt, max}$ is the battery capacity over the entire lifespan for normalizing the performance degradation. $\$_{batt}$ is the market price of the 80 V–40 Ah battery.

The inequality constraint $g(x,u)$ represents the physically allowable range for the current of the fuel cell system and the battery SOC, and the allowable changing rate of current of the fuel cell system:

$$i_{fc,min} \leq i_{fc} \leq i_{fc,max}, \ SOC_{batt,min} \leq SOC_{batt} \leq SOC_{batt,max}, \ \Delta i_{fc,min} \leq \frac{\Delta i_{fc}}{\Delta t} \leq \Delta i_{fc,max}, \qquad (14)$$

where Δi_{fc} is the change in the current of the fuel cell system from its previous value.

The boundary condition $h(x(t_0), x(t_f))$ represents the initial values of the current of the fuel cell system and the battery SOC:

$$i_{fc}(t_0) = i_{fc,init}, \ SOC_{batt}(t_0) = SOC_{batt,init}, \qquad (15)$$

where the initial current of the fuel cell system, $i_{fc,init}$, always starts from zero current. In other words, the DP calculates the optimal EMS with respect to the initial battery SOC, $SOC_{batt,init}$.

3.2. Trend Analysis of the Energy-Optimal Strategy

The trend analysis of the optimal EMS targets the DP results using two driving cycles, NEDC (New European driving cycle) and WLTC (Worldwide harmonized light vehicles test cycle) Class 2, as shown in Figure 4a. The NEDC cycle represents low-speed city driving and aggressive high-speed driving, and the WLTC Class 2 represents low and medium-speed city driving and high and extremely high-speed driving. Figure 4b shows the traction force F_{tract} calculated backward using the discretized version of the vehicle model (6) under the flat road grade assumption. The discretized time Δt is 0.1 s. The required conditions for DP are listed in Table 2.
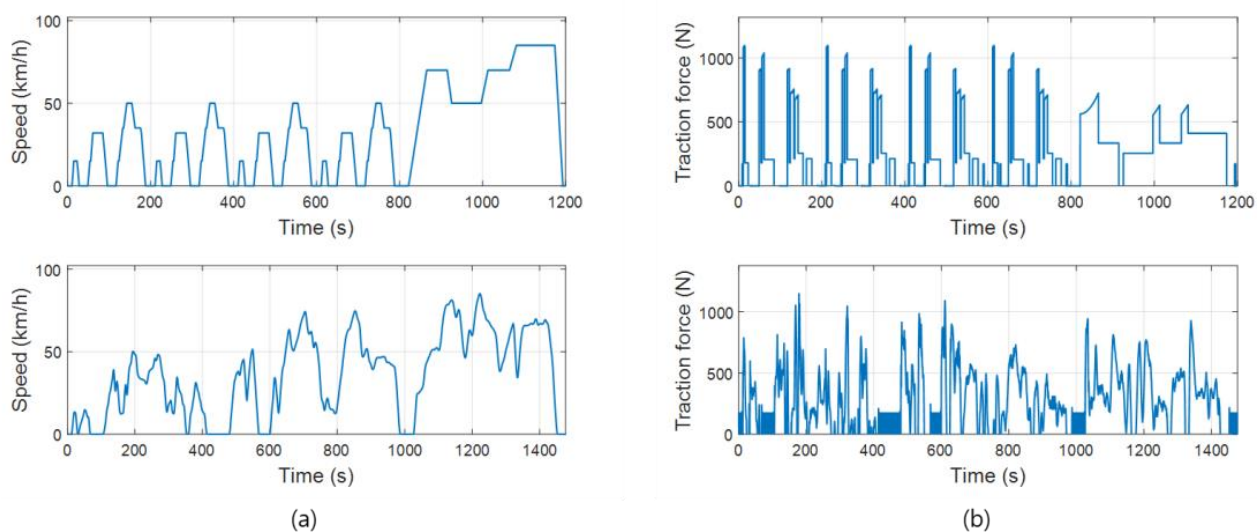

Figure 4. Driving cycles for the EMS design: (**a**) Driving cycle v_v; (**b**) Desired traction force F_{tract}.

Table 2. Conditions of the dynamic programming for analyzing optimal EMS trends.

		Symbol	Values
State discretization		i_{fc}	$-100{:}50{:}750$ A
		SOC_{batt}	$0.3{:}0.05{:}0.8$
Input discretization		m_{fc}	$0{:}0.1{:}1$
Cost function	J_{H2}	$\$_{H2}$	6.90 US\$/kgH$_2$ [1] [25]
	J_{FC}	w_{switch}	2.5×10^{-4}
		w_{power}	0.5×10^{-4}
		w_{perror}	4
		$\overline{P}_{fc}$	6000 W
		T_{FC}	8000 h [2] [26]
		$\$_{FC}$	560 US\$ [2] [26]
	J_{batt}	$w_{SOCbatt}$	3.25
		w_{charge}	0.45 ($i_{batt} \geq 0$), 0.55 ($i_{batt} < 0$)
		$\overline{i}_{batt}$	40 Ah
		$Q_{batt,\,max}$	15000×40 Ah
		$\$_{batt}$	720 US\$ [3] [27]
Inequality constraints		$i_{fc,\,min}$	0 A
		$i_{fc,\,max}$	4 A
		$SOC_{batt,\,min}$	0.3
		$SOC_{batt,\,max}$	0.8
		$\Delta i_{fc,\,min}$	-0.2 A/s
		$\Delta i_{fc,\,max}$	0.2 A/s

[1] based on 2025 US projection [25]. [2] based on 2025 US projection. The price of a fuel cell system is projected to be 35 USD/kW [26] [3] based on 2025 US projection. The price of a battery is projected to be 225 USD/kWh [27].

Figure 5 shows examples of the optimal EMSs obtained by the DP when the values of the initial battery SOC are 0.4, 0.55, and 0.7 for the two driving cycles, NEDC and WLTC. The top graphs represent the optimal modulation ratio of the fuel cell m_{fc}^*, i.e., the optimal EMS for the two driving cycles. The second and third graphs represent the states of the FCV with respect to the optimal EMS, i.e., the current of the fuel cell system and the battery SOC. Affluent initial battery SOC provides sufficient power to drive a vehicle without using the fuel cell system, and the fuel cell system is switched on when the battery SOC is insufficient. Table 3 lists the trip costs compared to a simple control strategy of switching on when the battery SOC drops to 0.4 and switching off when the battery SOC recharges to 0.7. The DP-based EMS significantly reduces the trip costs compared with the simple EMS, especially for the small initial battery SOC cases where many operations of the fuel cell system are required.
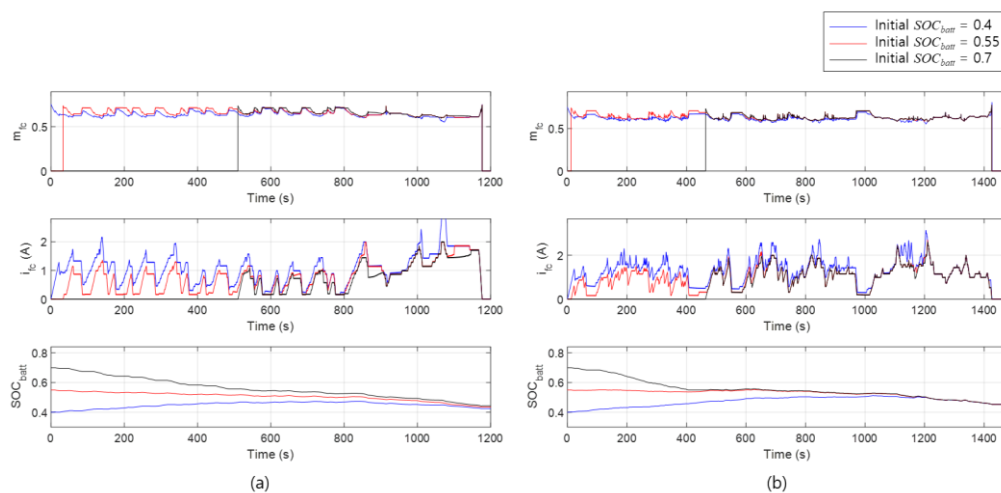
Figure 5. Dynamic programming results when the initial battery SOCs are 0.4, 0.55, and 0.7, respectively: (**a**) NEDC driving cycle; (**b**) WLTC driving cycle.

Table 3. Trip costs of the simple EMS and DP-based EMS.

Cycle Name	$SOC_{batt,init}$	Simple EMS (1)				DP-based EMS (2)				(1)–(2)
		J_{H2}($)	J_{FC}($)	J_{batt}($)	J($)	J_{H2}($)	J_{FC}($)	J_{batt}($)	J($)	J($)
NEDC	0.4	0.515	0.343	0.132	0.989	0.447	0.167	0.027	0.640	0.349
	0.55	0.453	0.188	0.124	0.765	0.345	0.170	0.025	0.539	0.226
	0.7	0.318	0.177	0.073	0.568	0.213	0.161	0.035	0.410	0.158
WLTC	0.4	0.857	0.372	0.165	1.394	0.629	0.169	0.037	0.836	0.558
	0.55	0.647	0.354	0.175	1.176	0.518	0.170	0.033	0.720	0.456
	0.7	0.617	0.202	0.117	0.937	0.383	0.162	0.044	0.589	0.347

The first step in designing an optimal energy management control strategy for an FCV is to find the maximum optimal current of the fuel cell system, i.e., maximum i_{fc}^*, for all optimal strategies in various initial battery SOCs. The maximum i_{fc}^* denotes the allowable range for the optimal current of the fuel cell system. Figure 6a displays the maximum i_{fc}^* with respect to the given power demand P_{demand} and the optimal battery SOC SOC_{batt}^* for all optimal strategies when the initial battery SOC ranges from 0.3 to 0.8.
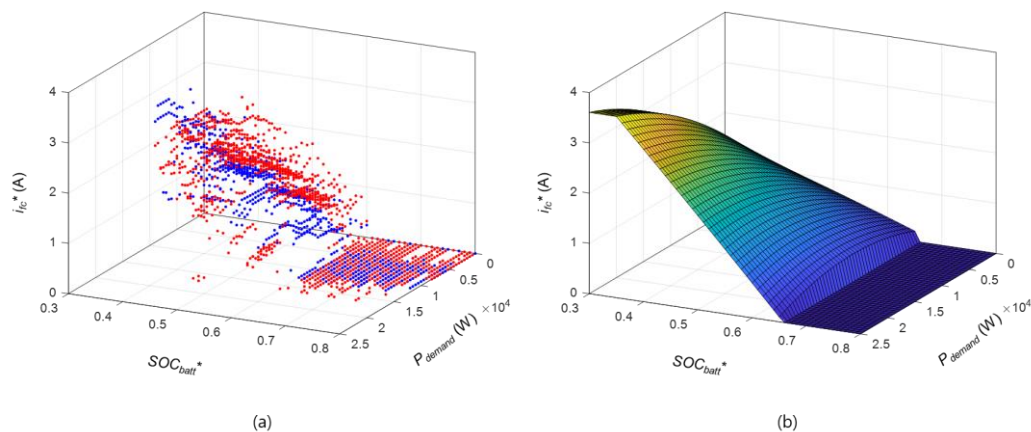

Figure 6. Allowable current of the fuel cell system for an optimal energy management control strategy: (**a**) Maximum i_{fc}^* with respect to the given P_{demand} and the SOC_{batt}^*(Blue color represents the NEDC cycle and red color represents the WLTC cycle); (**b**) Allowable i_{fc}^*.

Figure 6b shows the fitted curve of the maximum $i_{fc}*$ with respect to the given P_{demand} and the $SOC_{batt}*$. The maximum $i_{fc}*$ tends to be proportional to P_{demand} and inversely proportional to $SOC_{batt}*$ when $SOC_{batt}*$ is under 0.65. On the other hand, when $SOC_{batt}*$ exceeds 0.65, the maximum $i_{fc}*$ is zero, which denotes that the fuel cell system is switched off. Therefore, the overall allowable current of the fuel cell system to achieve the optimal energy management control strategy is as follows:

$$i_{fc} = \begin{cases} (aP_{demand} + 0.35b + c)^2, & SOC_{batt} < 0.35, \\ (aP_{demand} + bSOC_{batt} + c)^2, & 0.35 \leq SOC_{batt} \leq 0.65, \\ 0, & 0.65 < SOC_{batt} \end{cases} \qquad (16)$$

where *a*, *b*, and *c* are coefficients for the fitted curve.

3.3. Proposed Energy Management Control Strategy

An energy management control strategy should denote the modulation ratio of the fuel cell system with respect to the battery SOC and the power demand. Figure 7 shows the modulation ratio $m_{fc}*$ with respect to the given P_{demand} and the $SOC_{batt}*$, calculated using the allowable current of the fuel cell system $i_{fc}*$ and the fuel cell system dynamics (2). The modulation ratio can be defined within the allowable battery SOC after the fuel cell system is switched on, and its shape is proportional to $SOC_{batt}*$ and inversely proportional to P_{demand}. The decreased modulation ratio denotes the active operation of the fuel cell system. The fuel cell system is switched on when the battery SOC is under 0.65. Therefore, the modulation ratio is approximated by the functional structure of P_{demand} and the SOC_{batt} as follows:

$$m_{fc}* = \alpha - \beta\left(\frac{P_{demand}}{\overline{P}_{demand}}\right) - \gamma\left(1 - \frac{SOC_{batt}}{\overline{SOC}_{batt}}\right), \quad 0.3 \leq SOC_{batt} \leq 0.65, \qquad (17)$$

where $\overline{P}_{demand}$ and $\overline{SOC}_{batt}$ represent the nominal power demand and battery SOC for normalization, respectively. The coefficients α, β, and γ are defined as the optimized values, 0.7342, 0.3159, and 0.0559, using the particle swarm optimization (PSO) method optimizing the parameters by sharing the optimized solutions of each particle [28].
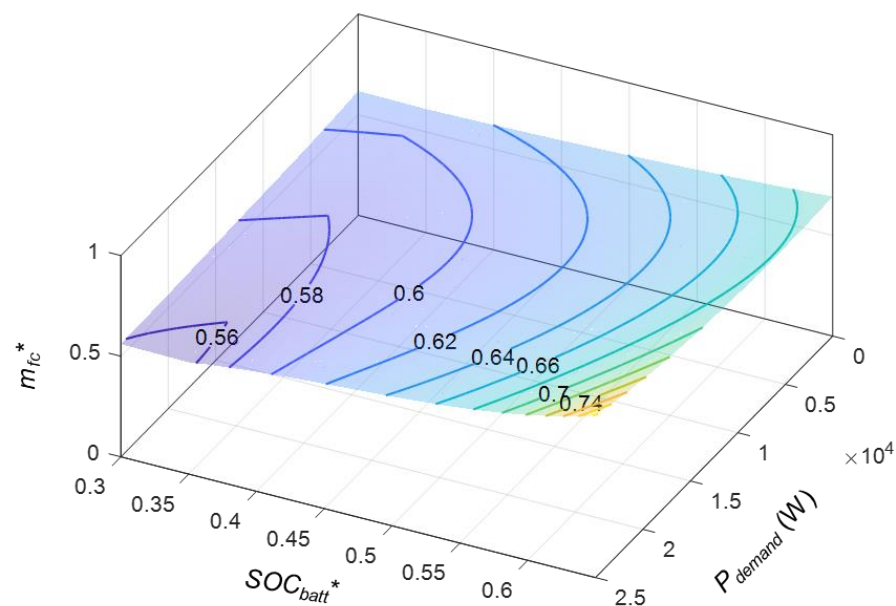

Figure 7. Modulation ratio $m_{fc}*$ with respect to the given P_{demand} and the $SOC_{batt}*$.

The proposed control strategy for an FCV involving both the fuel cell system on/off timing and the modulation ratio of the turned-on fuel cell system follows four governing rules based on the approximated modulation ratio function. First, the fuel cell system switches on when battery SOC is under 0.65. When the battery SOC exceeds 0.65, the modulation ratio is not defined, and the fuel cell system does not provide any current. Second, the modulation ratio for a turned-on fuel cell system operates as a function of the power demand and the battery SOC. The large power demand and the low battery SOC encourages the operation of the fuel cell system. Third, the fuel cell system switches off when the battery SOC recharges over 0.65. Lastly, the fuel cell system switches off for the continuous negative P_{demand} even after the modulation ratio becomes the standard value α. Therefore, the proposed control strategy is as follows:

$$FC : \begin{cases} switching\ on, & SOC_{batt} < 0.65\,, \\ m_{fc} = \alpha - \beta\left(\frac{P_{demand}}{P_{demand}}\right) - \gamma\left(1 - \frac{SOC_{batt}}{SOC_{batt}}\right), & SOC_{batt} \leq 0.65\,, \\ switching\ off & SOC_{batt} > 0.65 + \varepsilon\,, \\ switching\ off & P_{demand} < 0\ and\ m_{fc} = \alpha\,, \end{cases} \tag{18}$$

where ε is the allowable battery SOC to prevent switching chattering of the fuel cell system, calculated as 0.03 using the PSO method. Figure 8 shows the designed energy management control strategy.
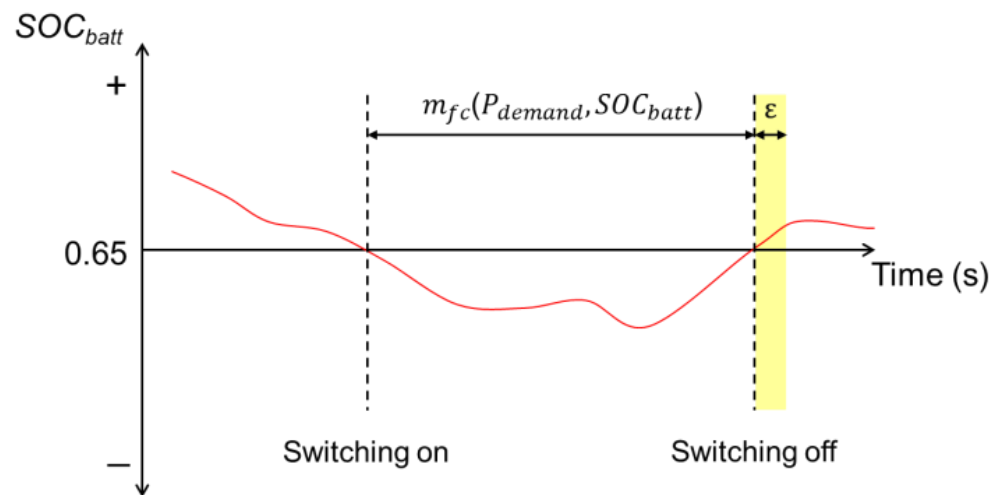

Figure 8. Proposed energy management strategy.

4. Validation

4.1. Performance Validation Compared to the DP

Figure 9 displays the results of the proposed EMS compared to the DP-based EMS for the NEDC driving cycle, one of the driving cycles utilized when the proposed EMS is generated. Results of the proposed EMS have different shapes to the DP-based results. On the other hand, trip costs of the proposed EMS are similar to those of the DP, as listed in Table 4. The DP-based EMS categorically reduces the trip cost the most, but requires information of the entire driving cycle. However, the proposed EMS can save trip costs without information of the entire driving cycle, which is more cost-effective than the simple EMS and similar to the DP-based optimal EMS. In particular, the proposed EMS shows good performance for the low initial battery SOC, which requires fast operation of the fuel cell system.
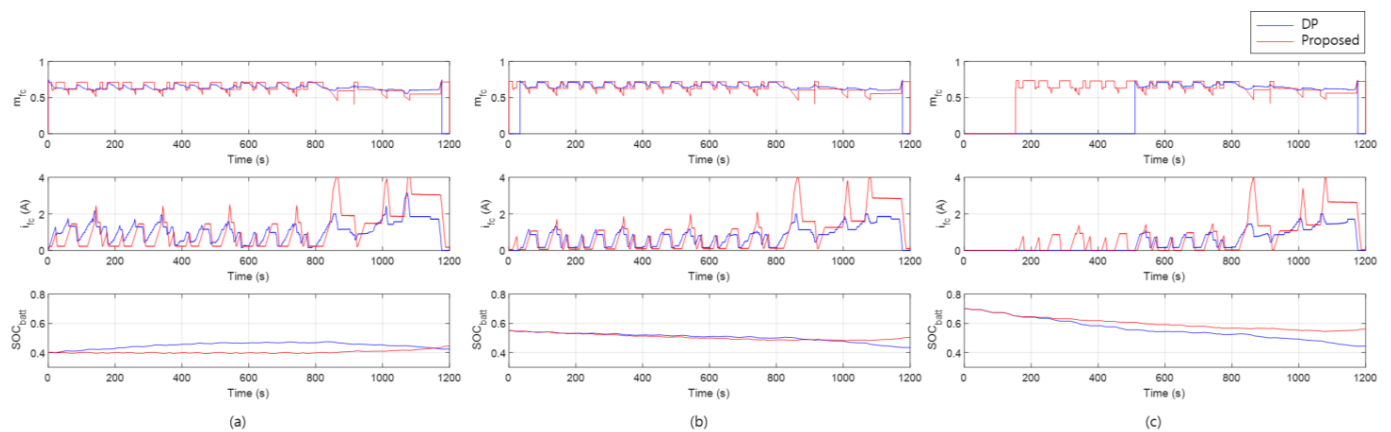
Figure 9. Results of the designed energy management control strategy for the NEDC cycle: (**a**) when the initial SOC is 0.4; (**b**) when the initial SOC is 0.55; (**c**) when the initial SOC is 0.7.

Table 4. Trip costs of the DP-based EMS and the proposed EMS.

Cycle Name	$SOC_{batt,init}$	DP-Based EMS (2)				Proposed EMS (3)				(2)–(3)
		$J_{H2}(\$)$	$J_{FC}(\$)$	$J_{batt}(\$)$	$J(\$)$	$J_{H2}(\$)$	$J_{FC}(\$)$	$J_{batt}(\$)$	$J(\$)$	$J(\$)$
NEDC	0.4	0.447	0.167	0.027	0.640	0.479	0.181	0.029	0.689	−0.049
	0.55	0.345	0.170	0.025	0.539	0.414	0.183	0.022	0.618	−0.079
	0.7	0.213	0.161	0.035	0.410	0.318	0.173	0.023	0.513	−0.103
WLTC	0.4	0.629	0.169	0.037	0.836	0.627	0.185	0.049	0.861	−0.025
	0.55	0.518	0.170	0.033	0.720	0.543	0.186	0.041	0.770	−0.049
	0.7	0.617	0.202	0.117	0.937	0.442	0.180	0.040	0.663	−0.074

4.2. Performance Validation for Other Driving Cycles

The proposed energy management control strategy using the optimal EMSs for NEDC and WLTC driving cycles was applied to other test cycles to guarantee robustness. Figure 10 shows the real driving cycles for testing and the desired traction force for the two cycles. The first test cycle represents mild city driving, and the second test cycle represents long-term driving with a mix of freeway and city driving. Table 5 lists the trip costs compared to the simple EMS-based strategy to switch the fuel cell system on and off at the battery SOC boundary conditions.
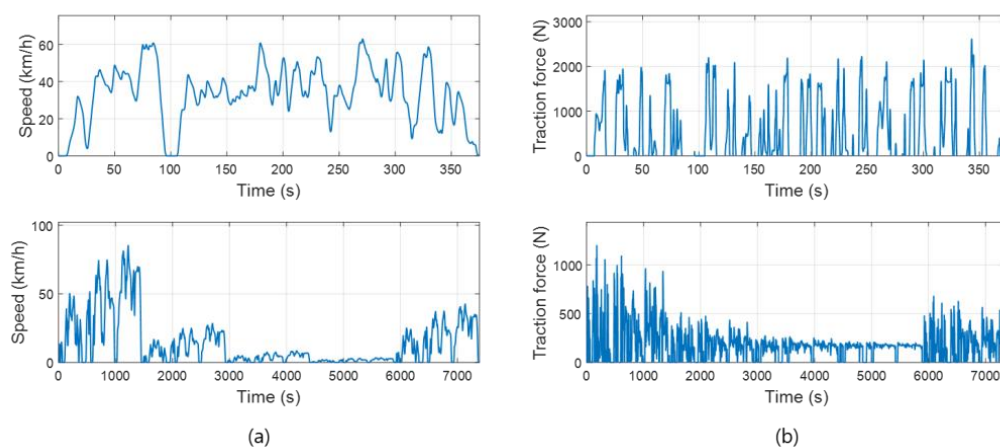

Figure 10. Test driving cycle for validation: (**a**) Driving cycle v_v; (**b**) Desired traction force F_{tract}.

Table 5. Trip costs of the simple EMS and the proposed-based EMS for the test cycles.

Cycle Name	$SOC_{batt,init}$	Simple EMS (1)				Proposed EMS (3)				(1)–(3)
		J_{H2}($)	J_{FC}($)	J_{batt}($)	J($)	J_{H2}($)	J_{FC}($)	J_{batt}($)	J($)	J($)
Test cycle 1	0.4	0.409	0.184	0.074	0.667	0.080	0.158	0.075	0.313	0.355
	0.55	0.122	0.160	0.077	0.359	0.062	0.160	0.060	0.282	0.077
	0.7	0	0	0.057	0.057	0.034	0.158	0.050	0.242	−0.184
Test cycle 2	0.4	2.779	1.132	0.579	4.490	2.337	0.280	0.087	2.704	1.786
	0.55	2.557	1.113	0.595	4.266	2.227	0.282	0.079	2.588	1.678
	0.7	2.374	0.948	0.516	3.838	2.100	0.278	0.080	2.457	1.381

For short trips with an affluent initial battery SOC, the simple EMS may save trip costs over the proposed method, as the battery is sufficient to drive the vehicle, and the fuel cell system does not need to be turned on, e.g., test cycle 1 with 0.7 $SOC_{batt,init}$ in Table 5. This result is natural as the vehicle uses only affordable electricity within the range where the battery life does not change dramatically without using the expensive hydrogen. However, all cases requiring the operation of the fuel cell system for recharging the battery or driving the vehicle show that the proposed EMS reduces trip costs over the simple EMS. The cost-effectiveness of the proposed EMS becomes pronounced with longer driving cycles, i.e., increased fuel cell operation due to increased battery consumption.

Table 6 shows the trip costs, the number of switching on of the fuel cell system N_{switch}, and the operating time of the fuel cell system t_{fc} for a driving cycle of about 10 days (888, 256 s) when the initial battery SOC $SOC_{batt,init}$ is 0.55. The maximum speed and power demand of the test cycle are 105.87 km/h and 31.73 kW, and the mean speed and power demand of the test cycle are 45 km/h and 7.87 kW, respectively. The long-term driving cycle accelerates obsolescence of the fuel cell system and battery, increasing trip costs related to the lifetimes of both systems significantly. Nevertheless, the proposed EMS can save two opposite trip costs related to the lifetimes of the fuel cell system and battery at the expense of a few hydrogen costs by reducing the switching on/off frequency of the fuel cell system and regulating the battery SOC. Therefore, the proposed EMS can be applied as a real-time control algorithm to save FCV trip costs associated with hydrogen consumption and obsolescence of both the fuel cell system and battery.

Table 6. Trip costs of the simple EMS and the proposed-based EMS for a 10-day driving cycle.

EMS Types	J_{H2}($)	J_{FC}($)	J_{batt}($)	J($)	N_{switch}	t_{fc}(%)
Simple	345.17	115.05	64.69	524.92	641	49.36
Proposed	354.30	16.61	28.82	399.73	1	99.98

5. Conclusions

This paper proposes an energy management control strategy to reduce trip costs of a fuel cell vehicle driving with two power sources: a fuel cell system and a battery. The trip cost involves the hydrogen consumption and lifetime of the two power sources. The design process of the energy management control strategy has three steps. First, the optimal energy management strategy is extracted through use of dynamic programming. Second, the allowable current of the fuel cell system is analyzed from the optimal strategies among various battery SOC conditions. Lastly, a strategy of both the fuel cell system on/off cycle and the modulation ratio of the turned-on fuel cell system is derived from the allowable current of the fuel cell system and fuel cell vehicle dynamics using the PSO algorithm. The proposed energy management control strategy was designed from the optimal strategies for two driving cycles and validated using two other cycles. The proposed control strategy reduces hydrogen usage while minimizing the aging of the fuel cell system and battery,

similar to the optimal strategy, but without requiring prior knowledge of future driving profiles yet remaining more cost-effective than the simple strategy of switching a fuel cell system on/off at the boundary conditions of the battery SOC.

However, the designed strategy bears three main limitations. First, the battery regeneration model was simplified. Second, the battery and the fuel cell system were simplified without reflecting obsolescence with respect to various disturbances, such as temperature. Last, the proposed control strategy was only taken into account for two driving cycles. In other words, the proposed control strategy may be inappropriate for other types of driving cycles where large amounts of battery regeneration may occur or obsolescence of the battery and the fuel cell system have progressed due to various disturbances. Therefore, future research intends to design a more robust energy management control strategy by strengthening the battery regeneration model and analyzing it at various cycles over a long-term period.

Author Contributions: Conceptualization, J.G.; methodology, M.K.; validation, M.K.; investigation, M.K.; data curation, J.G.; writing—original draft preparation, J.G.; writing—review and editing, C.A.; visualization, M.K.; supervision, C.A. All authors have read and agreed to the published version of the manuscript.

Institutional Review Board Statement: Not applicable.

Informed Consent Statement: Not applicable.

Data Availability Statement: Not applicable.

Conflicts of Interest: The authors declare no conflict of interest.

References

1. Wise, A. EPA Announces Tighter Fuel Economy Standards for Cars and Trucks. NPR Politics Newsletter, 2021. Available online: https://www.npr.org/2021/12/20/1066001919/epa-fuel-economy-standards-cars-trucks (accessed on 22 December 2021).
2. Bi, J.; Wang, Y.; Zhang, J. A data-based model for driving distance estimation of battery electric logistics vehicles. *EURASIP J. Wirel. Commun. Netw.* **2018**, *2018*, 251. [CrossRef]
3. Melo, P.; Araújo, R.E.; de Castro, R. Overview on Energy Management Strategies for Electric Vehicles—Modelling, Trends and Research Perspectives. In Proceedings of the International Youth Conference on Energetics, Leiria, Portugal, 7–9 July 2011; pp. 1–8.
4. Körner, A. Technology Roadmap-Hydrogen and Fuel Cells. In Proceedings of the International Energy Agency (IEA), Paris, France, 29 June 2015.
5. Sulaiman, N.; Hannan, M.A.; Mohamed, A.; Majlan, E.H.; Daud, W.W. A review on energy management system for fuel cell hybrid electric vehicle: Issues and challenges. *Renew. Sustain. Energy Rev.* **2015**, *52*, 802–814. [CrossRef]
6. Jiang, Z.; Chen, W.; Qu, Z.; Dai, C.; Cheng, Z. Energy management for a fuel cell hybrid vehicle. In Proceedings of the Asia-Pacific Power and Energy Engineering Conference, Chengdu, China, 28–31 March 2010; pp. 1–6.
7. Sundstrom, O.; Stefanopoulou, A. Optimal Power Split in Fuel Cell Hybrid Electric Vehicle with Different Battery Sizes, Drive Cycles, and Objectives. In Proceedings of the IEEE Conference on Computer Aided Control System Design, Munich, Germany, 4–6 October 2006; pp. 1681–1688.
8. Gharibeh, H.F.; Yazdankhah, A.S.; Azizian, M.R. Energy management of fuel cell electric vehicles based on working condition identification of energy storage systems, vehicle driving performance, and dynamic power factor. *J. Energy Storage* **2020**, *31*, 101760. [CrossRef]
9. Xin, W.; Zheng, W.; Qin, J.; Wei, S.; Ji, C. Energy management of fuel cell vehicles based on model prediction control using radial basis functions. *J. Sens.* **2021**, *2021*, 1–8. [CrossRef]
10. Liu, H.; Almansoori, A.; Fowler, M.; Elkamel, A. Analysis of Ontario's hydrogen economy demands from hydrogen fuel cell vehicles. *Int. J. Hydrogen Energy* **2012**, *37*, 8905–8916. [CrossRef]
11. Chen, H.; Pei, P.; Song, M. Lifetime prediction and the economic lifetime of Proton Exchange Membrane fuel cells. *Appl. Energy* **2015**, *142*, 154–163. [CrossRef]
12. Song, K.; Wang, Y.; Hu, X.; Cao, J. Online prediction of vehicular fuel cell residual lifetime based on adaptive extended Kalman filter. *Energies* **2020**, *13*, 6244. [CrossRef]
13. Hannan, M.A.; Hoque, M.M.; Mohamed, A.; Ayob, A. Review of energy storage systems for electric vehicle applications: Issues and challenges. *Renew. Sustain. Energy Rev.* **2017**, *69*, 771–789. [CrossRef]

14. Ouddah, N.; Boukhnifer, M.; Raisemche, A. Two Control Energy Management Schemes for Electrical Hybrid Vehicle. In Proceedings of the International Multi-Conferences on Systems, Signals & Devices, Hammamet, Tunisia, 18–21 March 2013; pp. 1–6.

15. Babazadeh, H.; Asghari, B.; Sharma, R. A new control scheme in a multi-battery management system for expanding microgrids. In Proceedings of the IEEE Innovative Smart Grid Technologies, Washington, DC, USA, 19–22 February 2014; pp. 1–5.

16. Hemi, H.; Ghouili, J.; Cheriti, A. A real time fuzzy logic power management strategy for a fuel cell vehicle. *Energy Convers. Manag.* **2014**, *80*, 63–70. [CrossRef]

17. RenHou, L.; Yi, Z. Fuzzy logic controller based on genetic algorithms. *Fuzzy Sets Syst.* **1996**, *83*, 1–10. [CrossRef]

18. He, H.; Zhang, Y.; Wan, F. Control Strategies Design for a Fuel Cell Hybrid Electric Vehicle. In Proceedings of the IEEE Vehicle Power and Propulsion Conference, Harbin, China, 3–5 September 2008; pp. 1–6.

19. Yu, S.; Zhang, J.; Wang, L. Power Management Strategy with Regenerative Braking for Fuel Cell Hybrid Electric Vehicle. In Proceedings of the Asia-Pacific Power and Energy Engineering Conference, Wuhan, China, 27–31 March 2009; pp. 1–4.

20. Xiao, D.; Wang, Q. The Research of Energy Management Strategy for Fuel Cell Hybrid Vehicle. In Proceedings of the International Conference on Industrial Control and Electronics Engineering, Xi'an, China, 23–25 August 2012; pp. 931–934.

21. Alloui, H.; Becherif, M.; Marouani, K. Modelling and Frequency Separation Energy Management of Fuel Cell-Battery Hybrid Sources System for Hybrid Electric Vehicle. In Proceedings of the Mediterranean Conference on Control and Automation, Platanias, Greece, 25–28 June 2013; pp. 646–651.

22. Depature, C.; Jemei, S.; Boulon, L.; Bouscayrol, A.; Marx, N.; Morando, S.; Castaings, A. IEEE VTS Motor Vehicles Challenge 2017—Energy Management of a Fuel Cell/Battery Vehicle. In Proceedings of the IEEE Vehicle Power and Propulsion Conference, 17–20 October 2016; pp. 1–6.

23. Bellman, R. Dynamic programming and stochastic control processes. *Inf. Control.* **1958**, *1*, 228–239. [CrossRef]

24. Hosen, M.S.; Jaguemont, J.; Van Mierlo, J.; Berecibar, M. Battery lifetime prediction and performance assessment of different modeling approaches. *IScience* **2021**, *24*, 102060. [CrossRef] [PubMed]

25. Jaganmohan, M. Levelized hydrogen costs at liquid stations in the U.S. 2017–2025. *Statista*. 2021. Available online: https://www.statista.com/statistics/1179532/us-levelized-hydrogen-costs-at-liquid-stations (accessed on 1 June 2021).

26. Bethoux, O. Hydrogen fuel cell road vehicles and their infrastructure: An option towards an environmentally friendly energy transition. *Energies* **2020**, *13*, 6132. [CrossRef]

27. Cole, W.; Frazier, A.W.; Augustine, C. *Cost Projections for Utility-Scale Battery Storage: 2021 Update*; National Renewable Energy Laboratory: Golden, CO, USA, 2021.

28. Meiying, Y.; Xiaodong, W. PSO-based parameter estimation of nonlinear systems. In Proceedings of the Chinese Control Conference, Zhangjiajie, China, 31 June–26 July 2007; pp. 533–536.